Cell

A Receptor-Modifying Deamidase in Complex with a Signaling Phosphatase Reveals Reciprocal Regulation

Xingjuan Chao,[1] Travis J. Muff,[3] Sang-Youn Park,[1] Sheng Zhang,[2] Abiola M. Pollard,[1] George W. Ordal,[3] Alexandrine M. Bilwes,[1] and Brian R. Crane[1,*]
[1] Department of Chemistry and Chemical Biology, Cornell University, Ithaca, NY 14853, USA
[2] Proteomics and Mass Spectrometry Core Facility, 143 Biotechnology Building, Ithaca, NY 14853, USA
[3] Department of Biochemistry, University of Illinois, Urbana, IL 61801, USA
*Contact: bc69@cornell.edu
DOI 10.1016/j.cell.2005.11.046

SUMMARY

Signal transduction underlying bacterial chemotaxis involves excitatory phosphorylation and feedback control through deamidation and methylation of sensory receptors. The structure of a complex between the signal-terminating phosphatase, CheC, and the receptor-modifying deamidase, CheD, reveals how CheC mimics receptor substrates to inhibit CheD and how CheD stimulates CheC phosphatase activity. CheD resembles other cysteine deamidases from bacterial pathogens that inactivate host Rho-GTPases. CheD not only deamidates receptor glutamine residues contained within a conserved structural motif but also hydrolyzes glutamyl-methylesters at select regulatory positions. Substituting Gln into the receptor motif of CheC turns the inhibitor into a CheD substrate. Phospho-CheY, the intracellular signal and CheC target, stabilizes the CheC:CheD complex and reduces availability of CheD. A point mutation that dissociates CheC from CheD impairs chemotaxis in vivo. Thus, CheC incorporates an element of an upstream receptor to influence both its own effect on receptor output and that of its binding partner, CheD.

INTRODUCTION

Reversible covalent modifications of transmembrane receptors regulate their ability to transmit signals across membranes in both eukaryotes and prokaryotes. Examples include ligand-induced reversible phosphorylation on Ser/Thr/Tyr residues (Roche et al., 1994; Schlessinger, 2002) and the reversible methylation of glutamate residues and deamidation of glutamine residues (Falke and Hazelbauer, 2001; Parkinson and Kofoid, 1992; Wadhams and Armitage, 2004). How specific sites on receptors are recognized by modification enzymes, and how modifications tune receptor activity, are largely unanswered questions. Well-characterized bacterial receptors that employ reversible demethylation/deamidation are the so-called Methyl-Accepting Chemotaxis Proteins (MCPs). These receptors sense the chemical environment and signal to the flagellar motor so that bacteria can adapt their swimming behavior appropriately. For some pathogenic bacteria, chemotaxis is critical for host colonization (Charon and Goldstein, 2002; Foynes et al., 2000).

MCP receptors span the membrane with two helical segments and interact with target small molecules via an extracellular domain of variable structure and a histidine kinase complex via a cytoplasmic domain that forms a striking 230 Å-long four-helix bundle (Falke and Hazelbauer, 2001). The region most distal to the membrane (the tip of the bundle) binds the effector histidine kinase CheA. The receptor-regulated histidine kinase phosphorylates the response regulator CheY, which diffuses from the receptor:kinase complex and binds to the flagellar switch complex. The direction of flagellar rotation (either clockwise CW or counterclockwise CCW) depends directly on the concentration of phosphorylated CheY (CheY-P) generated by CheA. In the absence of any change in the chemical environment, bacteria such as *B. subtilis* swim with a flagellar rotational bias of 55% CCW (Saulmon et al., 2004).

Kinase activity is modulated by the binding of extracellular ligands to receptors but also by receptor methylation. The methyltransferase CheR and the CheA-activated methylesterase CheB regulate the methylation state of MCPs in response to the stimulus level. This feedback control (adaptation) prevents signal saturation. In *E. coli*, CheB also deamidates selected Gln residues for subsequent methylation by CheR (Kehry et al., 1983). In *B. subtilis* (and presumably organisms with related chemotaxis machinery, such as the thermophile

T. maritima), both attractants and repellents stimulate demethylation of receptors, but the sites of modification differ (Zimmer et al., 2000).

In addition to CheB, most nonenteric chemotactic bacteria contain the chemotaxis protein, CheD, which will also deamidate specific Gln residues on MCPs (Kristich and Ordal, 2002). In *B. subtilis*, modification by CheD is essential for some MCPs to function in any capacity and for others to respond to appropriate ranges of extracellular ligand concentrations (Saulmon et al., 2004). Like null mutants of *cheA*, *cheY* and *cheR*, *cheD* null mutants are generally nonchemotactic in *B. subtilis* (Kirby et al., 2001; Rosario et al., 1995; Saulmon et al., 2004) and have a very low CCW bias (i.e., the mutant cells tumble most of the time). Also, *cheD* cells generate MCPs with abnormal levels of methylation (Kirby et al., 2001; Rosario et al., 1995).

In addition to its deamidase activity, CheD activates the aspartyl-phosphatase CheC (Park et al., 2004; Szurmant et al., 2004), which in vitro dephosphorylates CheY-P and thus acts downstream of the receptor to aid termination of the intracellular chemotaxis signal. However, in *B. subtilis*, CheY-P is primarily dephosphorylated by FliY, a CheC homolog that resides in the flagellar switch complex (Szurmant et al., 2003). The importance of FliY for CheY-P dephosphorylation is underscored by the severity of the *fliYΔ6-15* mutant, which produces a very high CCW bias because it cannot bind CheY-P. In contrast, the *cheC* null mutant has a nearly normal flagellar bias but a reduced frequency of switching (Saulmon et al., 2004). Nonetheless, *cheC* mutants respond poorly to certain attractants (2% of wt toward proline, and 30% of wt toward asparagine) (Kirby et al., 2001). Moreover, *cheC* mutants possess atypical MCP methylation levels and kinetics and do not adapt properly to some attractants (Rosario et al., 1995). The mechanisms by which CheC exerts these effects are not likely related to CheY-P dephosphorylation.

Herein we show that CheD represents an unusual class of deamidase, with a distant relationship to a family of bacterial toxins that function to deregulate host signaling proteins. The structure of the *T. maritima* CheC:CheD complex reveals that in addition to CheD activating CheC (Park et al., 2004; Szurmant et al., 2004), CheC inhibits CheD and thereby provides a potential intersection between the excitation phase of chemotaxis (mediated by CheY-P) and the adaptation response (mediated by receptor modification). To inhibit CheD, CheC incorporates a structural motif that mimics the CheD receptor substrate. This topologically variable region distinguishes CheC from other phosphatase family members, such as CheX and the flagellar protein FliY (Park et al., 2004; Szurmant et al., 2004). Mutations that disrupt the CheC:CheD complex in vivo, but not the enzymatic activities of either protein, impair chemotaxis. CheY-P stabilizes the CheC:CheD complex and thereby has the potential to downregulate receptor modification by CheD. Surprisingly, for the *T. maritima* proteins, the modification properties of CheD include demethylation of receptors that are not targets of CheB. The reciprocal regulation exhibited by the CheC:CheD complex may be a general strategy for temporally separating the activities of two components in a signaling network.

RESULTS AND DISCUSSION

CheD Resembles a Class of Bacterial Toxins

The structure of the *T. maritima* deamidase CheD (16 kDa) was determined in complex with the chemotaxis phosphatase CheC (22 kDa) and refined to 2.5 Å resolution (R factor 21%, R_{free} 27%; Table S1 available with this article online). The structure of CheD (Figure 1A) reveals a distant homology between CheD and a class of bacterial toxins represented by the cytotoxic necrotizing factor 1 (CNF1) (Buetow et al., 2001) (Figure 1B). The common fold consists of a three-layered α/β/β sandwich, wherein two mixed 5-stranded β sheets are flanked by a layer of two α helices. In a shallow cavity at the top of the α/β/β sandwich, an invariant Cys-His pair forms a catalytic dyad that is required by the toxins for deamidation activity (Buetow et al., 2001) (Figure 1). *E. coli* CNF1 constitutively activates host small G proteins such as Cdc42 and RhoA by deamidating a glutamine residue essential for GTP hydrolysis (Flatau et al., 2000; Schmidt et al., 1998). CheD also resembles a class of proteins of unknown function (represented by *B. subtilis* YfiH) that includes a human homolog (FLG38725). The structures for six of these proteins from *Caulobacter crescentus* (1XFJ), *Shigella flexneri* (1XAF and 1U05), *Bacillus stearothermophilus* (1T8H), *Neisseria meningitidis* (1RV9), and *Salmonella enterica* (1RW0) reveal a similar topology to that of CheD (Figure 1C). In addition to the Cys-His dyad, these proteins conserve another His residue not found in CheD or the toxins. The second conserved His acts with the Cys-His dyad to coordinate zinc in some of the structures (Figure 1C). The similarity in topology, sequence, and active center suggests an evolutionary relationship between CheD, CNF1, and the YfiH proteins, although due to the potential to bind zinc, reactivity of YfiH-like proteins may differ from that of CheD.

CheD Is a Cysteine Hydrolase

Other than CheD, site-specific deamidation is known to be catalyzed by CheB in bacterial chemotaxis (West et al., 1995) and the CNF family of toxins in bacterial pathogenesis (Buetow et al., 2001). Subcellular localization of protein kinase A also depends on Gln deamidation, but the deamidase has not yet been identified (Pepperkok et al., 2000). Based on residue conservation (Figure S1) and comparisons to CNF1, we evaluated conserved CheD residues for their ability to participate in the deamidation of *T. maritima* chemoreceptor cytoplasmic domains. Deamidation of receptors, which has been verified by high-resolution electrospray ionization tandem mass spectrometry (ESI/MS/MS, see below), results in a shift (slower migration) of the receptor band on SDS-PAGE (Figure 2A). Mutation of both the invariant Cys27 (to Ala, Asn, or His) and its hydrogen bonding partner His44 (to Ala) completely inactivates CheD (Figure 2A, lanes 2–4, 7). Mutation of Cys27 to Ala in CheD does not prevent CheD from binding MCP_{1143C} (Figure 2B). Mutation of conserved Ser26, directly adjacent to Cys27, results in complete

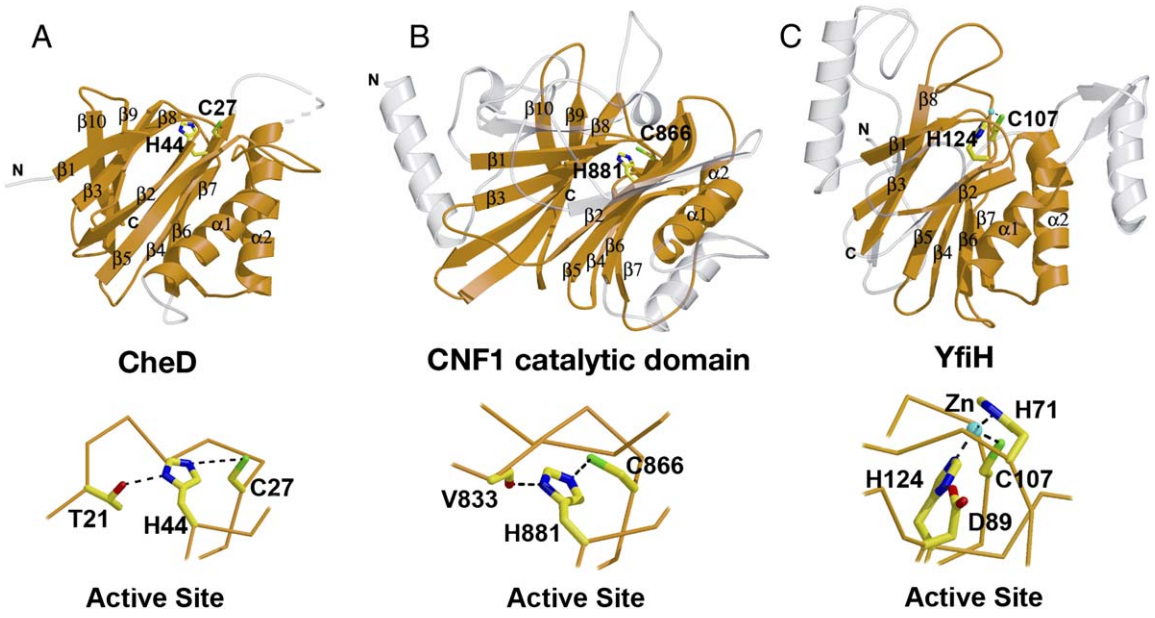

Figure 1. The Structures of CheD, CNF1 Catalytic Domain, and 1XAF

Folds and active site structures for (A) CheD, (B) CNF1 catalytic domain, and (C) *Shigella flexneri* YfiH. The three classes of proteins have common topologies (analogous regions in orange) but different peripheral loops and inserted regions (gray). CheD and CNF1 have similar active sites; YfiH incorporates an additional His ligand that allows zinc coordination.

loss of activity when changed to Ala (data not shown), but some activity is retained on change to Asn (Figure 2A, lane 5). Mutation of Thr21 to Ala, which also hydrogen bonds to His44, reduces activity by roughly 6-fold (Figure 2A, lanes 1 and 8, compare incubation times). CheD likely deamidates Gln residues with a mechanism analogous to that of cysteine proteases such as papain (Lorand and Graham, 2003; Stennicke and Salvesen, 1999). In this reaction, a nucleophilic thiol (Cys27) attacks the amide substrate at the carbonyl carbon, ammonia is lost, and a water molecule then hydrolyzes the remaining thioester. His44 is well positioned to facilitate the deprotonation of Cys27 and may also act as a proton donor to the amino-leaving group of the substrate. Thr21 stabilizes the positions of His44 and Cys27.

From a chemical standpoint, deamidation (in which an amide is converted to a carboxylate) closely relates to transamidation (in which the amine portion of the amide is replaced by another amine). Transglutaminases (TGs) catalyze crosslinking reactions between Gln residues and other amine donors, often Lys side chains. TGs are widespread and participate in many processes that include blood coagulation, extracellular matrix assembly, and modulation of the cytoskeleton (Lorand and Graham, 2003). Whereas TGs differ structurally from CheD and CNF1, they do conserve a papain-like catalytic triad of Asp-His-Cys and form a covalent thioester with substrate during catalysis (Lorand and Graham, 2003). Given the essential roles of CheD residues Cys27 and His44, such an intermediate is also likely formed by CheD during the deamidation reaction.

Even though some of the YfiH homologs employ the conserved Cys-His dyad to coordinate zinc, zinc is not required for deamidation of receptors by CheD (Figure S2). Crystallographic studies show that the CheD Cys-His dyad coordinates zinc when present at concentrations above 100 μM, but Zn^{2+} binding inhibits activity, as does binding by other divalent cations, including Ca^{2+} (Figure S2). In contrast, Ca^{2+} activates many Cys TGs (Lorand and Graham, 2003).

A Consensus Motif for CheD Target Sites

Evaluation of CheD substrate sites on cytoplasmic domains of three *T. maritima* MCPs (locus tags—TM1143, TM0429, and TM1428; respective carboxy-terminal cytoplasmic domains—residues 225–530, 347–656, 261–566) by ESI/MS/MS revealed a clear consensus sequence for CheD deamidation (Figure 3). In these experiments, peptides digested by trypsin are ionized by electrospray MS, fragmented by electron capture in an ion trap, and the resulting product ions are analyzed again by MS (Figure S3). On these three receptor domains, CheD deamidates 2 out of 16, 1 of 11, and 3 of 15 Gln residues, respectively. These sites all share key features: (1) the substrate Gln is either directly N-terminal or C-terminal to a Gln or Glu residue; (2) this Q E/Q motif always precedes the fully internal position in the coiled-coil; (3) the third residue preceding the first Gln in sequence and the third residue following the second Glu/Gln in sequence have small side chains (usually Ala and rarely Ser). There appears to be a strong requirement for the Ala residues; within the receptor substrates tested, deamidation of Gln residues next to Glu/Gln occurs only when the peripheral Ala residues are present. The crystallographic structure of the TM1143 cytoplasmic signaling domain, MCP_{1143C} (S.-Y.P., A.M.B., and B.R.C., unpublished data), reveals a 230 Å-long 4-helix

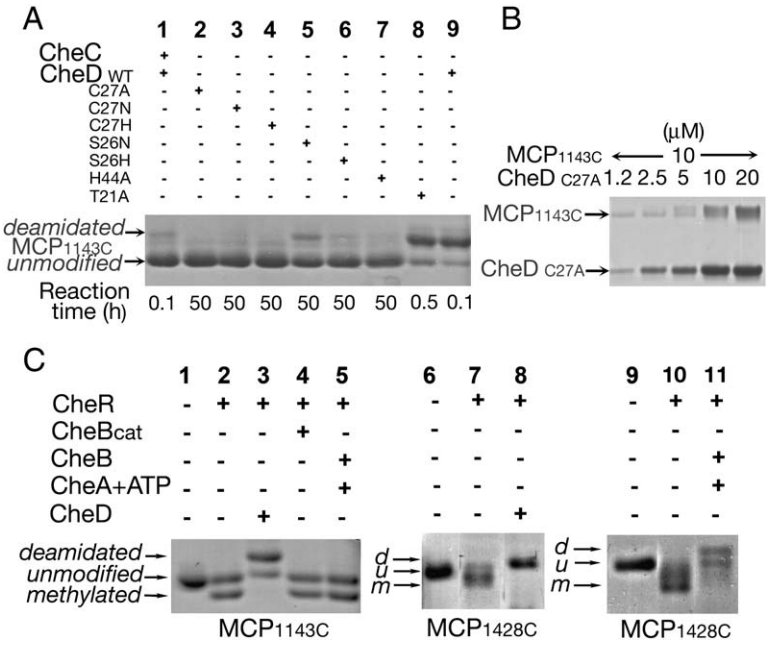

Figure 2. Activity and Affinity of *T. maritima* CheD and Variants toward Receptor Substrates; Comparison with *T. maritima* CheB

(A) Deamidation of the MCP_{1143C} receptor signaling domain results in an upshift on SDS-PAGE (coomassie stain). Two sites are deamidated (Q274 and Q498), but the upshift in mobility results primarily from Q274 (data not shown). CheD mutants C27A, C27N, C27H, H44A, and S26H are completely inactive, although CheD S26N retains some activity. CheD T21A requires a six times longer incubation to complete the reaction to the same extent as wild-type. CheC inhibits CheD when both proteins are present at 24 μM.

(B) Pulldown of MCP_{1143C} by various concentrations of His-tagged CheD mutant C27A bound to Ni-NTA agarose. This mutation of the CheD active site does not decrease the affinity of CheD for its substrate MCP_{1143C}.

(C) CheD and CheB act on different *T. maritima* receptors. In vitro deamidation and methylation/demethylation of MCP_{1143C} (lanes 1–5) and MCP_{1428C} (lanes 6–11) by CheD, CheR, and CheB. CheD deamidates and demethylates MCP_{1143C} and MCP_{1428C}. But, CheB only deamidates and demethylates MCP_{1428C}. Deamidated, unmodified, or methylated receptor domains display different migration of SDS-PAGE electrophoresis (Coomassie staining; see Experimental Procedures). CheB affects the migration of MCP_{1428C} but not that of MCP_{1143C}. Modifications were confirmed by MS (see Figures S3 and S5–S6).

coiled-coil (Figure 4B). The Glx-Glx deamidation sites project from two solvent-exposed positions along the helix, with the two Ala residues of the motif disposed one turn above and below the substrate sites (Figure 4B).

Proteins	Sequence Pattern								
		A/S	X	X	*Q/E*	*Q/E*	X	X	*A/S*
MCP1143C	*Site 274:*	*A*	S	V	Q	*E*	T	T	*A*
	Site 498:	*A*	R	L	Q	*E*	I	S	*A*
	Site 281:	*A*	G	S	E	*E*	I	S	*S*
	Site 505:	*A*	S	T	E	*E*	V	T	*S*
MCP1143C E499Q	*Site 498, 499:*	*A*	R	L	Q	Q	I	S	*A*
MCP1428C	*Site 282, 283:*	*A*	L	S	Q	Q	L	R	*S*
	Site 499:	*A*	S	A	Q	*E*	L	S	*A*
	Site 310:	*A*	S	I	E	*E*	V	T	*S*
	Site 317:	*S*	G	S	E	*E*	V	S	*A*
	Site 506:	*A*	A	S	E	*E*	M	S	*S*
MCP0429C	*Site 598:*	*A*	T	A	Q	*E*	Q	G	*A*
B. subtilis McpA	*Site 593, 594:*	*A*	T	V	Q	Q	L	S	*A*
CheC	*Site 150:*	*A*	I	F	A	E	A	S	I
CheC A150Q E151Q	*Site 150:*	*A*	I	F	Q	*Q*	A	S	I

Figure 3. Substrate Sites for CheD

The consensus sequence motif (top) that defines sites of deamidation (light gray Q) and demethylation (black E on gray circle) on receptors and CheC mutant. The deamidation sites of a *B. subtilis* McpA receptor also adheres to the consensus (Kristich and Ordal, 2002).

CheC Mimics the Receptor Substrate

Functional interaction between CheC and CheD was appreciated by the ability of CheD to stimulate CheC dephosphorylation activity in *Bacillus subtilis* (Szurmant et al., 2004) and *T. maritima* (Park et al., 2004). The structure of uncomplexed *T. maritima* CheC (Park et al., 2004) reveals internal 2-fold symmetry that relates the two halves of the protein. Two similar, but not identical, dephosphorylation centers were identified on helix α1 and symmetrically related helix α1′.

The structure of CheC in complex with CheD reveals how CheC binds CheD by inserting helix α2′ into the CheD active center (Figure 4A). Hence, the structure of the complex indicates that CheC inhibits CheD. In fact, CheC, which binds CheD with a dissociation constant K_D = 0.9-1.4 μM (Park et al., 2004), greatly curtails the deamidation activity of CheD (Figure 2A, lanes 1 and 9). Particularly striking, the CheC α2′ has the recognition motif contained in receptors except that Ala150 replaces the substrate Gln (Figure 4). Directly C-terminal to Ala150, the Glu151 side chain hydrogen bonds with conserved CheD Ser26 residue adjacent to the essential Cys27. Thus, Ser26 recognizes the Glx-Glx repeat in substrate sequences and positions the substrate amide next to Cys27. In CNF1, a conserved Ser residue (864) adjacent to the nucleophile Cys866 is also important for CNF1 to deamidate Rho G protein substrates (Buetow et al., 2001). Interestingly, CNF1 substrates, such as RhoA, Rac, and Cdc42 (Hoffmann and Schmidt, 2004), all conserve a Glu residue immediately C-terminal to the substrate Gln. Thus,

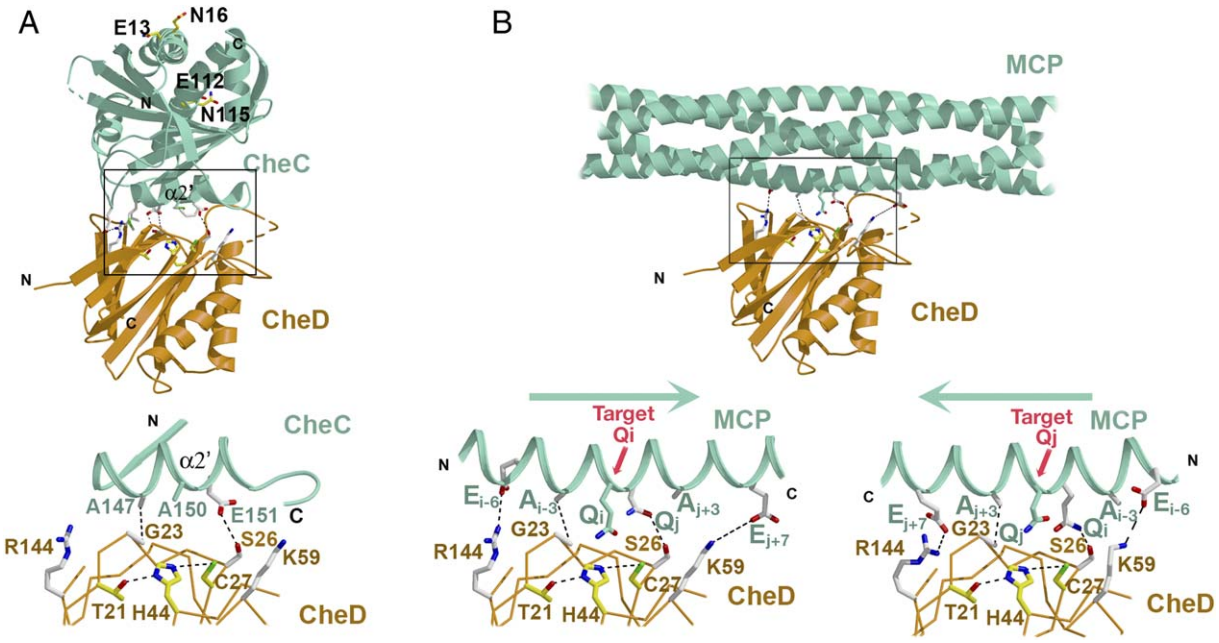

Figure 4. The CheC:CheD Complex Mimics the Receptor:CheD Interaction

(A) CheC (green) inserts α2′ into the CheD active center (orange) and blocks the catalytic center (yellow side chains). Residues involved in the phosphatase activity of CheC (E13, N16, E112, N115, yellow side chains) are peripheral from the interface. Expanded view of interface region (boxed, below) shows interactions (dotted lines) between key side chains (S26-to-E151, A147-to-G23, white) that mediate the contact. CheC A150 resides at the position of the substrate Gln in receptors.

(B) Ribbon diagram and expanded view (boxed, below) of the interaction between CheD and receptor MCP_{1143C} modeled on the structures of the CheD:CheC complex and the MCP_{1143C} receptor. CheC A150 is replaced by a substrate Gln. The symmetry of the receptor substrate likely allows CheD to bind to the helix in two directions and thereby maintain interaction of S26 with either Q_i or Q_j (below). The model predicts that CheD conserved residues R144 and K59 will engage acidic side chains often found peripheral to the receptor recognition motif at positions i − 6 or 7, j + 6 or 7.

the substrate recognition role of Ser864 in CNF1 may parallel that of Ser26 in CheD.

Interactions of CheC with CheD also reveal the role of conserved Ala residues in the recognition motif. Ala147 in CheC, one turn of helix N-terminal from the substrate position, packs directly against CheD Gly23 and Ala129; no large side chains could be accommodated at this position and maintain the helix contact (Figure 4). Organisms that contain both CheC and CheD in their genomes conserve both CheC Ala147 and CheD Gly23 (Figure S1). Mutation of either bracketing Ala residue on the MCP_{1143C} receptor to Phe greatly reduces the ability of CheD to deamidate Gln at either the N-terminal or C-terminal position in the tandem Gln/Gln site, with substitution at the C-terminal position causing the most drastic effect (Figure S4). Finally, two acidic residues usually flank the recognition motif on the receptors (three residues from the terminal Ala residues). The CheD:MCP model predicts that two conserved residues on CheD (Arg144 and Lys59) form salt bridges with these flanking carboxylates (Figure 4B).

Engineering CheC into a CheD Substrate

Demonstrating that CheC has co-opted the substrate recognition motif in order to inhibit CheD, installation of a Gln into CheC at position 150 results in its deamidation by CheD (Figure 5). However, CheD does not deamidate a tandem Gln at position 151 (Figure 4A). Thus, the additional interactions provided by CheC may prevent reorientation of the helix position in the CheD active site necessary for the deamidation of both Gln residues in the Gln-Gln repeat. Helix interactions in the CheD active center appear to prevent a shift of the substrate helix required for the deamidation of tandem Gln residues. For receptor substrates, CheD may bind the substrate helix in two different orientations with the helix direction running either N terminus-to-C terminus or visa versa through the CheD active center cleft (Figure 4B). Only by flipping the helix direction could interactions of Cys27 with the substrate Gln, and Ser26 with the nonsubstrate Gln/Glu, switch to allow deamidation of both residues. The symmetry of the recognition motif about the Glx-Glx tandem allows the CheD active center to accommodate the substrate helix in both directions (Figure 4B).

CheD Is also a Methylesterase

In *E. coli*, the CheB methylesterase deamidates Gln residues to glutamate but also hydrolytically demethylates the same residues after they have been converted to methyl esters by CheR (West et al., 1995). Consistent with a functional analogy to *E. coli* CheB, *T. maritima* CheD also demethylates *T. maritima* MCP_{1143C} and MCP_{1428C} after modification

Q

136-IDTLPPQLVIDMI**SAIF**E**QA**SIEELEDNSEDQIVFVETLLK-176

b ion	residue	calculated Mass	experimental Data	experimental mass minus calculated
b14	**Ser**	1536.8	1537.1	0.3
b15	**Ala**	1607.9	1608.1	0.2
b16	**Ile**	1721.0	/	/
b17	**Phe**	1868.0	1868.2	0.2
b18	**Gln**	*1996.1*	*1997.2*	*1.1*
b19	**Gln**	2124.1	2125.2	*1.1*
b20	**Ala**	2195.2	2196.2	*1.0*

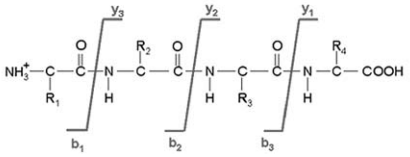

Figure 5. CheD Deamidates CheC when Gln Is Introduced at the Substrate Site

ESI/MS/MS spectrum analysis of triply charged ion at *m/z* 1549.2 from the CheC A150Q-E151Q double mutant treated with CheD. A tryptic peptide (residues 136 to 176, top) encompassing the 150 region gains mass of 1 Da at residue 150. Gln151 is not deamidated by CheD. Peptides fragments as y and b ion series are defined below.

by *T. maritima* CheR (Figures 2C and 3 and Figure S5). MS-MS analysis shows that MCP_{1143C} contains two major methylation sites per subunit (E. Perez, H. Zheng, and Ann Stock, personal communication [Rutgers University, New Jersey]), whereas MCP_{1428C} contains three (Figures 2C and 3 and Figure S6). CheD hydrolyzes all methyl esters added by CheR on these two receptor domains (Figure 2C and Figure S5). Not surprisingly, the MCP methylation sites fit the CheD recognition motif (Figure 3). Thus, the cellular role of CheD likely involves receptor deamidation, regulation of the CheC phosphatase, but also participation in the adaptation response manifested through the reversible methylation/demethylation of receptors. Moreover, *T. maritima* CheB, when activated by CheA, will not demethylate CheR-treated MCP_{1143C} in vitro but will demethylate another *T. maritima* receptor, MCP_{1428C} (Figure 2C). Activated CheB removes methyl groups from four sites on MCP_{1428C} (three major and one minor; Figure 2C and Figure S6). Thus, CheB and CheD have distinct substrate sites on different receptors with some overlap in specificity. These differential in vitro activities parallel the differential effects of CheD on various *B. subtilis* receptors. For example, the *B. subtilis cheD* mutant still responds to asparagine (through McpB) but not to proline (through McpC) (Kirby et al., 2001). Furthermore, the CheD dependence of McpC, which does not depend on deamidation, is lost in a chimeric McpC that contains a portion of McpB outside the deamidation region (the so-called HAMP domain) (Kristich and Ordal, 2004). Furthermore, McpA, whose ligands are not known, appears highly methylated in the *cheD* mutant (Kristich and Ordal, 2002). Thus, CheD targets receptors differentially and has activities other than receptor deamidation. CheC and CheD are often cotranscribed, and in *B. subtilis* CheC has been shown to be expressed at low copy number (~20 proteins per cell, compared to >800 McPs) (Szurmant et al., 2004). Thus, functions of CheD are likely enzymatic and include demethylation of some receptors, such as *T. maritima* MCP_{1143} and possibly *B. subtilis* McpA.

Activation of CheC by CheD

CheD modifies receptors and thereby tunes their ability to produce the chemotaxis signal CheY-phosphate (CheY-P). CheC dephosphorylates CheY-P. The association of CheC with CheD inhibits CheD but also activates CheC, providing an intersection of function within the signaling network. CheD could activate CheC by two general mechanisms. Either CheD allosterically influences CheC, or the CheC:CheD complex aids recognition of CheY-P. Essential residues for CheC phosphatase activity reside on the pseudosymmetric helices α1 and α1′ that stretch across the side of the central β sheet opposite to α2′ and are therefore peripheral to the CheC:CheD interface (Figure 6A). A conserved Pro-Pro motif on the edge strand juxtaposes invariant and catalytically essential Asn residues on α1 and α1′. Due to its internal pseudosymmetry, CheC has two clusters of these residues; mutations of the two symmetry-related asparagine residues (13 and 115) are required to abrogate activity (Park et al., 2004). Binding of CheD to CheC results in no significant structural changes in the active center residues, but modeling of *T. maritima* CheY-P in contact with the second (more active) CheC active site indicates that an exposed surface loop of CheD between β6 and α2 (residues 94 to 99) will likely contact CheY as it engages the conserved cluster of CheC residues on α1′ and β1′ (Figure 6C). Directly N-terminal to this exposed loop, Met92 and Phe93 on CheD insert into a hydrophobic pocket on CheC (composed of Val141, Ile148, and the aliphatic side chains of Gln139 and Lys64). In the genome sequences of organisms that contain CheC and CheD, Met92 and Phe93 are conserved in 20 of 22 cases (for the two exceptions the sequence is Ile-Phe; Figure S1). Thus, the Met-Phe sequence is a strong indication of a conserved CheC:CheD interaction and the succeeding exposed loop is well positioned to aid in CheY recognition.

To test the ability of CheD to stabilize a complex between CheC and CheY-P, we evaluated the influence of CheY and CheY-P on receptor deamidation by CheD in the presence of CheC. After long incubation times (required because CheD activity in the presence of CheC is low), CheY-P, but not CheY, further inhibited receptor deamidation by CheD (Figure 6D). Thus, CheY-P stabilizes the CheC:CheD complex, which indicates that the CheC:CheD complex has a higher affinity than CheC alone for CheY-P (Figure 6A). Importantly, this result implies that high CheY-P levels will reduce availability of enzymatically active CheD.

CheX, which has the same fold and activity as CheC, shows greater CheY phosphatase activity than CheC but,

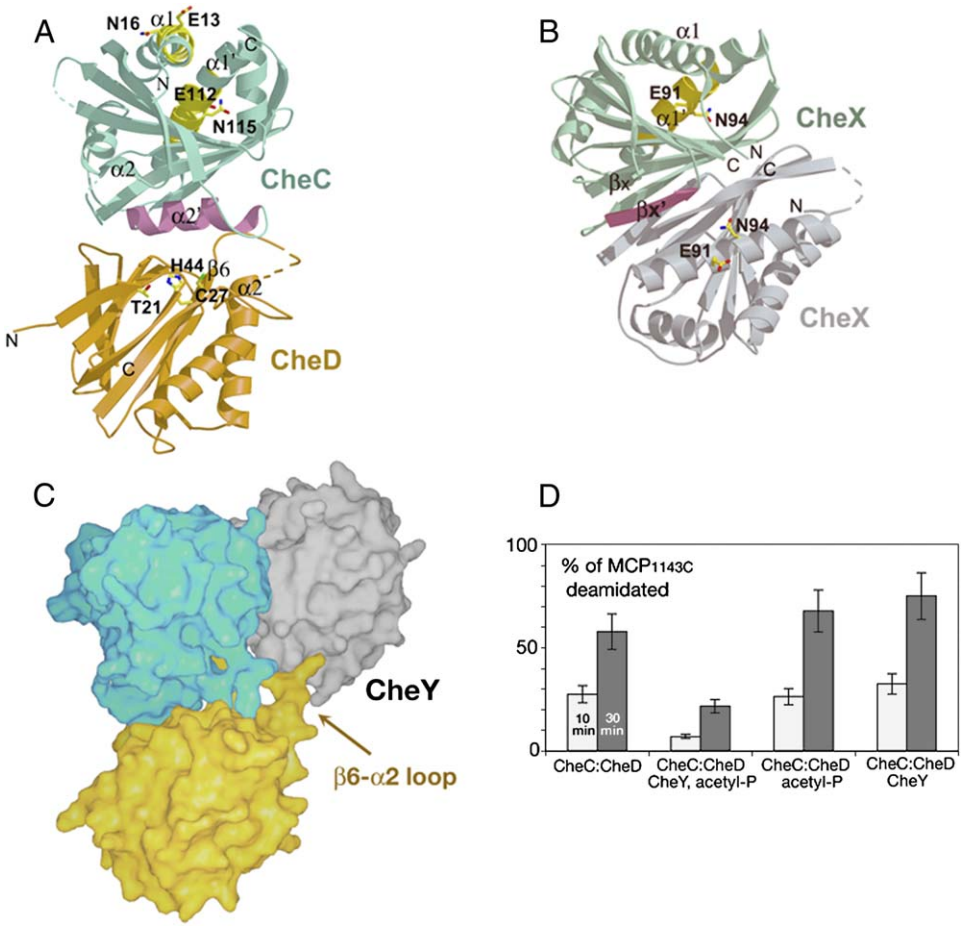

Figure 6. CheC and CheX Employ Analogous Regions of Different Structure to Mediate Complex Formation

(A) In the CheC:CheD heterodimer, the CheC α2′ region (magenta) binds CheD and thereby orients important residues in CheC activity away from the interface. A loop region between CheD β6 and α2 (residues 94–99) may interact with CheY-P and increase its affinity for binding CheC.

(B) In CheX, the β_x' (magenta) replaces CheC α2′ and forms a continuous β strand at the CheX homodimer interface.

(C) Space-filled representation of a putative CheC:CheD (green:orange) complex with CheY (gray) based on a reasonable alignment of CheY and CheC active site residues. This arrangement allows for contacts between CheD loop β6-α2 and CheY.

(D) CheY-P, but not CheY, inhibits the deamidation activity of CheD in the presence of CheC. Bands representing deamidated and nondeamidated MCP_{1143C} were quantified by Coomassie blue staining on SDS gels, followed by densitometry with software Image J. The percentage of product, i.e., deamidated MCP_{1143C}, is shown as a function of two incubation times (10 and 30 min). Error bars represent the mean ± the standard error (σ_m).

unlike CheC, is an obligate dimer (Park et al., 2004) (Figure 6B). In CheX, a β strand that mediates dimerization replaces CheC α2′. Associating CheY-P with the conserved active residue cluster on the CheX subunit indicates that the adjacent subunit will likely aid in binding CheY-P. Thus, CheC and CheX have a variable secondary structure element that for CheC mediates binding to CheD but for CheX mediates dimerization. CheC then incorporates a structural motif into its fold that mimics a CheD substrate recognition site to bait and inactivate the deamidase while at the same time generating an improved interaction surface for its own substrate, CheY-P. Thus, the CheC:CheD complex reveals an unusual mechanism for how two proteins can simultaneously act as positive and negative regulators for each other and link circuits in a signaling network.

Breaking the CheC:CheD Complex Impairs Chemotaxis

Based on the CheC:CheD crystal structure, Asp149 in the α2′ CheD recognition helix of *B. subtilis* CheC was mutated to Lys to disfavor complex formation with CheD. In vitro, the CheC mutant dephosphorylates CheY-P at normal levels in the absence of CheD but shows little activation on the addition of CheD (Figure 7A). A *cheC* mutant strain complemented with Asp149Lys CheC showed severely reduced chemotaxis in a traditional swarm plate assay, similar to the *cheC* null (Figure 7B). Pulldown experiments demonstrate that the affinity of CheC for CheD has been substantially reduced by the mutation (Figure 7C). Thus, the activation of CheC requires binding of CheD to α2′ in vivo, and formation of the CheC:CheD complex is essential for robust chemotaxis.

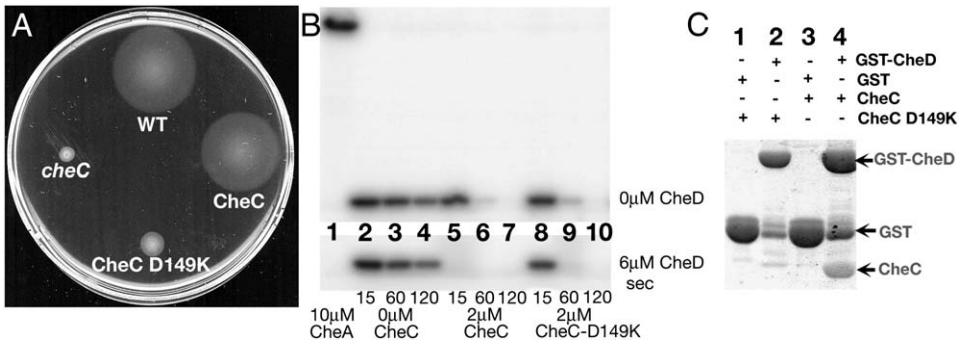

Figure 7. A *cheC* Mutant Defective in Binding CheD Shows Impaired Chemotaxis in *B. subtilis*

(A) Swarm plate assay. From top going clockwise is wild-type *B. subtilis* (OI1085), the *cheC* deletion with pMR130 (integration plasmid containing cheC) (OI3165), the D149K mutant in the same construct as OI3165, and the *cheC* deletion (OI3135). The swarm diameters of OI3135, OI4172, and OI3165 are 20%, 30%, and 90% of the wild-type swarm diameter, respectively. The mutant CheC functions slightly, but chemotaxis is severely curtailed.

(B) CheY-P hydrolysis assay: shown are time points (15, 60, 120 s) tracking dephosphorylation of CheY-P. Lane 1 contains CheA-P before the addition of 20 μM CheY. The enhancement of the CheY-P hydrolysis activity of CheC by CheD is almost entirely lost in the CheC D149K mutant (compare lanes 5 and 8 in lower gel).

(C) Pulldown assay to confirm that the CheC D149K mutant no longer binds CheD.

CheD Provides a Pathway for Receptors to Respond to CheY-P Levels

With the exception of enterobacteria and ϵ-proteobacteria, most chemotactic prokaryotes contain CheD (Figure S1). In *B. subtilis*, mutation of *cheD* produces a drastic phenotype, similar to null mutants of the two central signaling components *cheA* and *cheY*. CheD has enzymatic activities that include receptor deamidation, receptor demethylation, and activation of the CheY phosphatase CheC. Furthermore, we have shown that CheD and CheB operate on different receptor target sites in *T. maritima*. In well-studied *B. subtilis*, which has a chemotaxis system much closer to *T. maritima* than that of enteric bacteria, methylation on different receptor sites can have opposing effects on kinase activity (Zimmer et al., 2000). In many bacteria, the *cheC* and *cheD* genes lie adjacent and nest within the same transcript, perhaps to ensure coordinated expression of their protein products. The CheC:CheD complex, in addition to activating CheC, inhibits the enzymatic activity of CheD. This complex then provides a mechanism by which receptor modification states can respond directly to CheY-P levels. If cellular copy numbers of the proteins are indeed low (as suggested by CheC quantification in *B. subtilis* [Szurmant et al., 2004]), the dissociation constant of the complex (~1 μM in *T. maritima* [Park et al., 2004]) may allow for significant levels of free CheC and CheD. However, high CheY-P levels will stabilize CheD within the inhibitory CheC:CheD complex. Hence, receptors sites and CheY-P levels may compete to control CheD availability. Moreover, the conditions that favor free CheD (low CheY-P, low CheA activity) are opposite to those that favor high CheB activity (high CheY-P, high CheA activity). This provides a means to differentially regulate two receptor-modifying enzymes of differing substrate specificity. In *B. subtilis*, CheY has been shown to affect receptor remethylation during adaptation by an unknown mechanism (Kirby et al., 1999) that may involve the CheC:CheD complex. Reverse effects on the activities of the CheC and CheD proteins in their mutual complex allow temporal separation of their enzymatic functions in response to CheY-P levels. Reciprocal regulation of two components in the same pathway by simple hetero-oligomerization is an attractive means to regulate interconnected signaling loops and one that may well extend beyond bacterial chemotaxis.

EXPERIMENTAL PROCEDURES

Protein Preparation (*T. maritima*)

The genes encoding *T. maritima* CheC, CheD, CheR, CheB, CheA, CheY, MCP_{1143C}, MCP_{1428C}, MCP_{0429C}, and their mutants were PCR cloned into the vector pET28a (Novagen) and expressed with a 6-His tag in *E. coli* strain BL21 (DE3) (Novagen). Recombinant colonies were grown in Terrific Broth (DIFCO) with kanamycin selection (25 μg/ml). The CheC, CheD, and MCP_{1143C} point mutations were introduced by QuickChange mutagenesis (Stratagene) and verified by sequencing. All proteins were purified on separate Nickel-NTA agarose columns (Qiagen). Wild-type CheC, CheD, MCP_{1143C}, MCP_{0429C}, and MCP_{1428C} were digested by human thrombin (Haematologic Technologies Inc.) to remove their His-tag. All proteins were further purified by sizing chromatography (Amersham Biosciences Superdex 75) and concentrated by centrifugation (Amicon Centriprep) in GF buffer (50 mM Tris [pH 7.5] and 150 mM NaCl). Subsequently, CheC and CheD were mixed at 1:1.2 ratio and purified again by gel filtration. The CheC:CheD complex was concentrated by centrifugation in GF buffer to around 100 mg/ml as measured by UV absorbance at 280 nm.

Crystallization and Data Collection

Crystals of CheC:CheD complex (~100 mg/ml) grew by vapor diffusion against a reservoir of 0.25 M Lithium Sulfate, 0.1 M Tris (pH 7.5), 0.1M cesium chloride, and 30% PEG 4000. The crystals belong to the space group $P3_2$ and contain two CheC:CheD complexes per asymmetric unit. Native diffraction data were collected to 2.4 Å resolution at CHESS beamline F2 (Table S1).

Structure Determination and Refinement

The structure was determined by molecular replacement with AMoRe (Navaza, 1994) using CheC (PDB code 1XKR) as a probe (starting correlation coefficient 0.228). The asymmetric unit comprises two CheC/CheD

complexes. The CheD model was manually built from 2Fo-Fc and Fo-Fc electron density maps in XFIT (McRee, 1992). Many iterations between manual rebuilding and CNS refinement (Brunger et al., 1998) were necessary to obtain a complete and accurate model. As the original probe contained only a fraction of the unit cell and none of CheD, model building necessitated the extensive use of omit maps and noncrystallographic symmetry averaging to confirm loop connections. The final model was refined to 2.4 Å (R factor 21.1% and R_{free} 27.5%; Table S1) and shows good agreement with the electron density and acceptable protein stereochemistry. The model includes CheC residues 1 to 203 (out of 205), CheD residues 1 to 157, and 392 water molecules; CheC surface loop 176–178 and CheD surface loop 147–151 are disordered in both molecules (Table S1).

In Vitro Deamidation Assays of *T. maritima* MCPs

MCP_{1143C} (20–30 μM) and CheD or CheC:CheD complex (20–30 μM) were incubated in GF buffer (15 μl as the final volume) at 37ºC for 5 min or 30 min, respectively. For CheD mutants, concentrations of 30–40 μM were used and the incubation time was lengthened to 30 min (for CheD T21A) or 50 hr (for all other six CheD mutants). MCP_{1143C} mutants (A271F_Q498A, A278F_Q498A, A271F_QE274EQ_Q498A, A278F_QE274EQ_Q498A) were incubated with wild-type CheD as above and products were analyzed in time courses that ranged 1–50 hr. For assays with *T. maritima* CheB, 20–30 μM CheB was added along with 4–5 μM CheA and 1.0 mM Mg-ATP. The reactions were stopped by adding 6 μl of 4× SDS loading buffer and heated at 80ºC for 10 min. Samples were centrifuged and divided into 15 and 5 μl aliquots. The larger volumes were loaded onto 20 cm long 12% SDS-PAGE gel and electrophoresed at 80 volts for 24 hr to resolve the difference in migration between deamidated and native receptors, whereas the smaller volume samples were loaded onto SDS-PAGE mini gels and ran at 200 volts for 35 min to visualize and quantify the amount of receptor and CheD present.

In Vitro Deamidation Assays in the Presence of CheY

MCP_{1143C} (20–30 μM) samples were incubated in GF buffer supplemented with $MgCl_2$ 125 μM for about 1 min at 37ºC following the addition of CheY (250–300 μM) and/or acetyl phosphate (acetyl-P) 500 μM. Subsequently, CheC:CheD (20–30 μM) was added to the samples, which were then incubated at 37ºC (75 μl as the final total volume). At 10 min and 30 min, 30 μl of reaction solution was quenched with SDS loading buffer and analyzed by electrophoresis, as described above.

In Vitro Demethylation Assays of *T. maritima* MCPs

MCP_{1143C} (20–30 μM), CheR (20–30 μM), and 200 μM S-adenosylmethionine (SAM) were incubated in GF buffer (30 μl as the final volume) at 37ºC for 1–2 hr. The reactions were split into two vials. 20–30 μM of CheD (or 20–30 μM CheB with 4–5 μM CheA and 1.0 mM ATP) was added into one of the vials. Both vials were incubated at 37ºC for another 30 min. The reactions were stopped by adding 6 μl of 4× SDS loading buffer and heated at 80ºC for 10 min. Samples were centrifuged and divided into 15 and 5 μl aliquots. The larger volumes were loaded onto 20 cm long 12% SDS-PAGE gel and electrophoresed at 80 volts for 24 hr to resolve the difference in migration between methylated and native receptors, whereas the smaller volume samples were loaded onto SDS-PAGE mini gels and ran at 200 volts for 35 min to visualize and quantify the amount of receptor, CheR, and CheD.

T. maritima CheD-MCP Pulldown Assays

Ten micromoles of MCP_{1143C} were incubated at 37ºC for 30 min with either 1.2, 2.5, 5, 10, or 20 μM His-tagged CheD C27A bound to 20 μl Ni-NTA agarose beads previously equilibrated in binding buffer (25 mM Hepes [pH 7.5], 0.5 M NaCl, 5 mM Imidazole). Beads were washed four times with 1 ml washing buffer (25 mM Hepes [pH 7.5], 0.5 M NaCl, 20 mM Imidozole), centrifuged, and the supernatant removed. The beads were then mixed with 6 μl SDS sample loading buffer and heated at 80ºC for 10 min prior to SDS-PAGE electrophoresis analysis.

Identification of *T. maritima* MCP Modification Sites by Mass Spectrometry

Modified trypsin was from Promega (Madison, WI) and sequence grade chymotrypsin was purchased from Sigma (St. Louis, MO). All other chemical reagents, unless otherwise noted, were obtained from Aldrich (Milwaukee, WI).

Protein Tryptic Digestion

Protein samples were desalted by using either Micron filter unit from Millipore (Bedford, MA) for buffer exchange to 25 μM ammonium bicarbonate (pH 7.8) or a Slide-A-Lyzer Mini Dialysis Unit from Pierce (Rockford, IL) for dialysis overnight at 4ºC. One hundred microliters of 1 μg/μl receptor was digested by 1 mg/ml trypsin (Promega, Madison, WI) at 37ºC for 24 hr at a 1:60 ratio (w/w) for MCP_{1428} and 1:10 ratio (w/w) for MCP_{1143C} and CheC. For the CheC A150Q mutant, the tryptic digest was followed by adding 1 mg/ml chymotrypsin at 1:10 ratio (w/w) and incubated at 37ºC for an additional 24 hr. To overcome the high acidity of the receptors, additional buffer was sometimes added to obtain the proper pH range for proteolysis.

Infusion Electrospray Mass Spectrometric Analysis

All enzymatic digest samples were diluted to a concentration of 500 fmol to 1 pmol/μl in 50% acetonitrile with 0.1% formic acid prior to MS analysis. Each sample was delivered with a syringe pump to a hybrid triple quadrupole linear ion trap mass spectrometer equipped with a 4000 Q Trap and Turbo V source from ABI/MDS Sciex (Framingham, MA). The flow rate of sample delivery was 4 μl/min. The sample was analyzed in both tune mode and information-dependant acquisition (IDA) mode with Analyst 1.4 software. A 5 kV spray voltage, nitrogen curtain (10 psi), and collision gas (set to high) with a heated interface were used for all experiments. The declustering potential (DP) was set at 40 V to minimize in-source fragmentation. The 4000 Q Trap was operated in positive LIT-mode at enhanced MS (EMS) for survey scan (*m/z* 400–1700) and enhanced product ion (EPI) for MS/MS scans (*m/z* 100–2800). The scan speed was set to 1000 Da/s and at least 2 min of data (over 50 scans) were summed for each spectrum. The collision energy was 35–60 eV in EPI scan for different peptide ions. The trap fill-time was either 10 ms in the EMS mode or 20 ms in EPI scan mode. The ion source nebulizer gas and turbo gas were set up to 25 psi and 30 psi, respectively. In IDA analysis, an EMS of *m/z* 450 to *m/z* 1600 followed by an enhanced resolution (ER) scan and three EPI scans with rolling collision energy was performed for a 5 min acquisition on each sample.

Data Analysis

The MS/MS data generated from both EPI scan and IDA analysis were submitted to Mascot 1.9 for database searching against the Mass Spectrometry protein sequencing database (MSDB). One missed cleavage site was allowed. The peptide tolerance was set to 2 Da and MS/MS tolerance was set to 0.8 Da. A deamination modification of asparagine and glutamine residues was set as variable modification. For the MS/MS spectra on the tryptic peptides containing mutant residues, the data were interpreted manually using Analyst 1.4 and BioAnalyst 1.4 software (Applied Biosystem).

Mutagenesis and Strain Construction

Strains OI1085 (wild-type); OI3135, a null mutant in *cheC*; and OI3165, which is OI3135 complemented with wild-type *cheC* (using pMR130, which is pDR67::*cheC*) were described previously (Rosario et al., 1995). Strain OI4172 is the same as OI3165 but with the CheC-D149K mutation. The *Bacillus subtilis cheC-D149K* mutant was created by Quickchange mutagenesis (Stratagene) of *cheC* on plasmid pMR108 (Rosario et al., 1995). The mutant gene was subcloned into pGEX-6P-2 for GST-tagging and overexpression in *E. coli* as described (Szurmant et al., 2004).

Dephosphorylation Assay

Assay was performed essentially as described (Szurmant et al., 2004). *B. subtilis* chemotaxis proteins were purified by GST-tag from *E. coli*

cultures, and the GST-tag was subsequently removed (Szurmant et al., 2004). Fifty micromoles CheA was phosphorylated by incubation with [γ-^{32}P]ATP (1 μCi/μl) for 6 min in TKMD (50 mM Tris, pH 8; 5 mM $MgCl_2$, 50 mM KCl, 0.2 mM dithiothreitol, 10% glycerol). The ^{32}P-labeled CheA was then diluted to 10 μM in the reaction mixture of 20 μM CheY, 5 mM cold ATP, in the presence or absence of 2 μM CheC, 2 μM CheC-D149K, 6 μM CheD in TKMD buffer. Time points were taken at 15 s, 1 min, and 2 min and the reaction stopped by addition of 2× SDS buffer with 100 mM EDTA. Samples were separated on 12% SDS-PAGE, exposed to a storage phosphor-screen (Molecular Dynamics), and the image taken with a Storm 860 Phosphor imager (Amersham Bioscience).

GST Pulldown for *B. subtilis* Proteins

The experiment was performed using Handee Spin Cup Columns (Pierce) and centrifuge spins were done at 1000 × g for 30 s. All wash steps were performed with 400 μl PBS/Triton (20 mM Na_2HPO_4, pH 7.5, 150 mM NaCl, 1% Triton X-100). Fifty microliters of glutathione beads (Amersham) were washed twice before 100 μl of GST or GST-CheD was added to a concentration of 80 μM. The sample was incubated for 10 min at room temperature and washed twice. Then, 100 μl of the secondary protein (CheC or CheC-D149K) was added to a concentration of 100 μM, incubated 10 min, and washed four times. The sample was eluted following addition of 75 μl of Buffer GEB (50 mM Tris, pH 8.0, 10 mM glutathione) and incubation for 10 min. After centrifugation, 25 μl of SDS solubilizer buffer was added to the sample and 10 μl of that sample was run on SDS-PAGE and Coomassie blue stained.

Swarm Plate Chemotaxis Assay

Assay was performed essentially as described (Szurmant et al., 2004). Single colonies of *B. subtilis* strains tested were picked from TBAB plates grown 16 hr at 30ºC, inoculated onto semi-solid swarm plates (1% tryptone, 0.5% NaCl, 0.3% agar) with 1 mM IPTG for expression of *cheC* and *cheC-D149K* from pDR67, and grown at 37ºC for 6 hr.

Computer Graphics

Figures 1, 4, and 6 were rendered by Molscript (Kraulis, 1991) and Raster3D (Merritt and Murphy, 1994). Figure S2 was made with Bobscript (Esnouf, 1997).

Supplemental Data

Supplemental data include six figures and one table and can be found with this article online at http://www.cell.com/cgi/content/full/124/3/561/DC1/.

ACKNOWLEDGMENTS

We thank Richard Cerione for helpful discussions; the Cornell High Energy Synchrotron Source for access to data collection facilities; the Cornell University Mass-spectrometry facility; Eduardo Perez, Haiyan Zheng, and Ann Stock for sharing data prior to publication; Bryan Beel for supplying the CheR construct; and Gabriela Gonzalez-Bonet for supplying receptor proteins. X.C. thanks a Tsang Fellowship for financial support. This work was supported by NIH grants GM054365 to G.W.O. and GM066775 to B.R.C.

Received: June 4, 2005
Revised: September 22, 2005
Accepted: November 15, 2005
Published: February 9, 2006

REFERENCES

Brunger, A.T., Adams, P.D., Clore, G.M., Delano, W.L., Gros, P., Grosse-Kunstleve, R.W., Jiang, J.S., Kuszewski, J., Nilges, M., Pannu, N.S., et al. (1998). Crystallography and NMR system: a new software suite for macromolecular structure determination. Acta Crystallogr. *D54*, 905–921.

Buetow, L., Flatau, G., Chiu, K., Boquet, P., and Ghosh, P. (2001). Structure of the Rho-activating domain of Escherichia coli cytotoxic necrotizing factor 1. Nat. Struct. Biol. *8*, 584–588.

Charon, N.W., and Goldstein, S.F. (2002). Genetics of motility and chemotaxis of a fascinating group of bacteria: the spirochetes. Annu. Rev. Genet. *36*, 47–73.

Esnouf, R.M. (1997). An extensively modified version of Molscript that includes greatly enhanced coloring capabilities. J. Mol. Graph. *15*, 133–138.

Falke, J.J., and Hazelbauer, G.L. (2001). Transmembrane signaling in bacterial chemoreceptors. Trends Biochem. Sci. *26*, 257–265.

Flatau, G., Landraud, L., Boquet, P., Bruzzone, M., and Munro, P. (2000). Deamidation of RhoA glutamine 63 by the Escherichia coli CNF1 toxin requires a short sequence of the GTPase switch 2 domain. Biochem. Biophys. Res. Commun. *267*, 588–592.

Foynes, S., Dorrell, N., Ward, S.J., Stabler, R.A., McColm, A.A., Rycroft, A.N., and Wren, B.W. (2000). Helicobacter pylori possesses two CheY response regulators and a histidine kinase sensor, CheA, which are essential for chemotaxis and colonization of the gastric mucosa. Infect. Immun. *68*, 2016–2023.

Hoffmann, C., and Schmidt, G. (2004). CNF and DNT. Rev. Physiol. Biochem. Pharmacol. *152*, 49–63.

Kehry, M.R., Bond, M.W., Hunkapiller, M.W., and Dahlquist, F.W. (1983). Enzymatic deamidation of methyl-accepting chemotaxis proteins in Escherichia coli catalyzed by the cheB gene product. Proc. Natl. Acad. Sci. USA *80*, 3599–3603.

Kirby, J.R., Saulmon, M.M., Kristich, C.J., and Ordal, G.W. (1999). CheY-dependent methylation of the asparagine receptor, McpB, during chemotaxis in Bacillus subtilis. J. Biol. Chem. *274*, 11092–11100.

Kirby, J.R., Kristich, C.J., Saulmon, M.M., Zimmer, M.A., Garrity, L.F., Zhulin, I.B., and Ordal, G.W. (2001). CheC is related to the family of flagellar switch proteins and acts independently from CheD to control chemotaxis in *Bacillus subtilis*. Mol. Microbiol. *42*, 573–585.

Kraulis, P.J. (1991). Molscript: a program to produce both detailed and schematic plots of protein structures. J. Appl. Crystallogr. *24*, 946–950.

Kristich, C.J., and Ordal, G.W. (2002). Bacillus subtilis CheD is a chemoreceptor modification enzyme required for chemotaxis. J. Biol. Chem. *277*, 25356–25362.

Kristich, C.J., and Ordal, G.W. (2004). Analysis of chimeric chemoreceptors in Bacillus subtilis reveals a role for CheD in the function of the McpC HAMP domain. J. Bacteriol. *186*, 5950–5955.

Lorand, L., and Graham, R.M. (2003). Transglutaminases: crosslinking enzymes with pleiotropic functions. Nat. Rev. Mol. Cell Biol. *4*, 140–156.

McRee, D.E. (1992). XtalView: a visual protein crystallographic software system for X11/Xview. J. Mol. Graph. *10*, 44–47.

Merritt, E.A., and Murphy, M.E.P. (1994). Raster3D Version 2.0: a program for photorealistic molecular graphics. Acta Crystallogr. *D50*, 869–873.

Navaza, J. (1994). AMoRe: an automated package for molecular replacement. Acta Crystallogr. *A50*, 157–163.

Park, S.Y., Chao, X., Gonzalez-Bonet, G., Beel, B.D., Bilwes, A.M., and Crane, B.R. (2004). Structure and function of a unusual family of protein phosphatases: the bacterial chemotaxis proteins CheC and CheX. Mol. Cell *16*, 563–574.

Parkinson, J.S., and Kofoid, E.C. (1992). Communication modules in bacterial signaling proteins. Annu. Rev. Genet. *26*, 71–112.

Pepperkok, R., Hotz-Wagenblatt, A., Konig, N., Girod, A., Bossemeyer, D., and Kinzel, V. (2000). Intracellular distribution of mammalian protein kinase A catalytic subunit altered by conserved Asn2 deamidation. J. Cell Biol. *148*, 715–726.

Roche, K.W., Tingley, W.G., and Huganir, R.L. (1994). Glutamate receptor phosphorylation and synaptic plasticity. Curr. Opin. Neurobiol. *4*, 383–388.

Rosario, M.M., Kirby, J.R., Bochar, D.A., and Ordal, G.W. (1995). Chemotactic methylation and behavior in Bacillus subtilis: role of two unique proteins, CheC and CheD. Biochemistry *34*, 3823–3831.

Saulmon, M.M., Karatan, E., and Ordal, G.W. (2004). Effect of loss of CheC and other adaptational proteins on chemotactic behaviour in Bacillus subtilis. Microbiol. *150*, 581–589.

Schlessinger, J. (2002). Ligand-induced, receptor-mediated dimerization and activation of EGF receptor. Cell *110*, 669–672.

Schmidt, G., Selzer, J., Lerm, M., and Aktories, K. (1998). The Rho-deamidating cytotoxic necrotizing factor 1 from Escherichia coli possesses transglutaminase activity. Cysteine 866 and histidine 881 are essential for enzyme activity. J. Biol. Chem. *273*, 13669–13674.

Stennicke, H.R., and Salvesen, G.S. (1999). Catalytic properties of the caspases. Cell Death Differ. *6*, 1054–1059.

Szurmant, H., Bunn, M.W., Cannistraro, V.J., and Ordal, G.W. (2003). Bacillus subtilis hydrolyzes CheY-P at the location of its action, the flagellar switch. J. Biol. Chem. *278*, 48611–48616.

Szurmant, H., Muff, T.J., and Ordal, G.W. (2004). Bacillus subtilis CheC and FliY are members of a novel class of CheY-P-hydrolyzing proteins in the chemotactic signal transduction cascade. J. Biol. Chem. *279*, 21787–21792.

Wadhams, G.H., and Armitage, J.P. (2004). Making sense of it all: bacterial chemotaxis. Nat. Rev. Mol. Cell Biol. *5*, 1024–1037.

West, A.H., Martinez-Hackert, E., and Stock, A.M. (1995). Crystal structure of the catalytic domain of the chemotaxis receptor methylesterase, CheB. J. Mol. Biol. *250*, 276–290.

Zimmer, M.A., Tiu, J., Collins, M.A., and Ordal, G.W. (2000). Selective methylation changes on the Bacillus subtilis chemotaxis receptor McpB promote adaptation. J. Biol. Chem. *275*, 24264–24272.

Accession Numbers

The coordinates reported herein have been deposited with the Protein Data Bank with accession number 2F9Z.